Structure, Dissociation Energies, and Harmonic Frequencies of Small Doubly Charged Carbon Clusters C_n^{2+} ($n = 3-9$)†

Sergio Díaz-Tendero, Fernando Martín,* and Manuel Alcamí

Departamento de Química, C-9, Universidad Autónoma de Madrid, 28049-Madrid, Spain

Received: March 20, 2002; In Final Form: May 30, 2002

We have studied the structure of small doubly charged carbon clusters using density functional (DFT) and coupled-cluster (CC) theories. We have found that, with the exception of C_4^{2+} and C_7^{2+}, the most stable geometry corresponds to linear structures of $D_{\infty h}$ symmetry. This is at variance with the behavior observed in neutral and singly charged carbon clusters. We have also evaluated dissociation energies corresponding to various dissociation channels that are useful in mass spectrometry experiments. This requires that absolute energies of neutral and singly charged species are evaluated at the same level of theory. As a byproduct of the latter calculations, we have evaluated first and second ionization potentials that are still unavailable in the literature. Harmonic frequencies for the doubly charged species have been also evaluated.

1. Introduction

The properties of small carbon clusters have been the subject of intense theoretical and experimental research in the past decade (see, e.g., a recent review by Van Orden and Saykally,[1] and references therein). Carbon clusters of various sizes have been identified in the interstellar space,[2−5] but they can also be produced in the laboratory, e.g., by laser vaporization of graphite followed by a supersonic expansion into an inert carrier gas. Neutral, anionic, and cationic carbon clusters form directly from the laser initiated plasma in sizes ranging from one to hundreds of atoms. The size distribution produced in these plasmas can be controlled at will by varying various experimental parameters, such as laser power, gas pressure, temperature, the geometry of the supersonic nozzle, and so forth. Nowadays selection of clusters with a well-defined number of atoms is possible for almost any size. This has led to a tremendous progress in the determination of microscopic properties of these clusters (atomization energies, ionization potentials, structures, harmonic frequencies, and so forth) and has guided the theory in a similar direction.

Theoretical information exists for almost any neutral species.[1,6−16] Not only accurate energies have been obtained from high level calculations for sizes up to $n = 10$, but also structures and vibrational spectra have been characterized thoroughly. Among the large number of theoretical papers devoted to these systems, it is important to mention the work of Martin and Taylor[11,12,15] who have performed the most extensive calculations of structural, rotational, vibrational, and electronic properties of neutral carbon clusters C_n using coupled cluster methods including all single and double excitations and a quasi-perturbative treatment of connected triple excitations CCSD(T).

Positively charged carbon clusters C_n^{q+} have been much less studied. In this case, traditional spectroscopic methods are more difficult to apply. Therefore, one must often rely on theoretical data. Nevertheless some experimental investigations have been carried out for singly ionized clusters based, e.g., on gas-phase ion chromatography[17,18] or diverse variants of spectroscopic,[19,20] spectrometric[21−27] or Coulomb explosion techniques.[28] Singly ionized carbon clusters have been theoretically investigated in a recent work by Giuffreda et al.[29] using density functional theory, DFT, and CCSD(T) methods. The latter authors have performed an extensive study of structural and vibrational properties of linear and cyclic carbon clusters C_n^+ with $n = 4-19$, and have found results compatible with a few available experimental data**.** An additional information that arises from their study is the first ionization potential of the parent neutral species. The ionization potentials obtained by Giuffreda et al.[29] systematically disagree with experimental data by more than 1 eV. These authors attribute the origin of the discrepancy to the fact that the experimental values[30−34] may correspond to the vertical ionization potentials instead of to the adiabatic ones. Nevertheless, further investigations are needed to clarify this point.

Information on small highly ionized carbon clusters is much scarcer. This is not the case in the context of fullerene research, since doubly positively charged C_{60}^{2+} is known to be stable against Coulomb explosion since the early nineties (see for instance[35,36]). The latter discovery triggered a series of experimental activities and, by now, the existence of higher charged species C_n^{q+} with $n = 56$, 60, 70 has been clearly established up to $q = 7$.[37] In contrast with fullerenes, the search of small highly ionized carbon clusters has not been initiated until very recently. The most basic question to be answered in this field is the following: what is the minimum size a carbon cluster must have in order to be stable against Coulomb explosion for a given value of charge q? Wohrer and collaborators[38−42] have recently shed some light into this problem. They have produced highly ionized carbon clusters, C_n^{q+} with $q \geq 2$, in collisions of fast singly ionized carbon clusters impinging on a helium gas. Processes leading to multiply charged clusters are single and multiple ionization, which, at high impact energies, are more efficient than neutralization.[38] Preliminary results obtained in 1997[39] suggest the existence of a doubly charged C_5^{2+} cluster whose lifetime is larger than the time-of-flight window used in the experiment (50 ns). They also suggest that excited C_5^{2+}

† Part of the special issue "R. Stephen Berry Festschrift".

* To whom correspondence should be addressed. E-mail: fernando.martin@uam.es.

10.1021/jp0257956 CCC: $22.00
Published on Web 08/13/2002

clusters mainly decay to $C_4^+ + C^+$ and not to $C_3^+ + C_2^+$, in contrast with metal clusters for which the dominant fission channels are those leading to almost symmetric fragments.[43] More recent experiments[41] show that the measured multiionization cross section leading to highly charged (HC) species depend significantly on the initial cluster geometry, being favored those HC clusters that are initially in a cyclic configuration.

Despite the growing experimental interest on small doubly ionized carbon clusters C_n^{2+}, nothing is known about their electronic and vibrational properties or about their stability against Coulomb explosion for $n > 5$. A preliminary study on the energetics of doubly charged carbon clusters with $n \leq 5$ has been reported in reference.[44] Hogreve[45,46] has evaluated the potential energy surfaces, PES, of C_3^{2+} and C_4^{2+} by using multireference configuration interaction methods. He has found that both clusters are metastable, i.e., they are associated to local minima in the PES with energy larger than that of the separate fragments. However, the local minima are "protected" by large and wide barriers, so that even the smallest C_3^{2+} cluster is pretty stable against dissociative tunneling.[45] C_3^{2+} is linear with a $^1\Sigma_g^+$ ground state,[45] while linear and cyclic geometries are nearly isoenergetic for C_4^{2+}.[46] Obviously, the stability of doubly charged clusters should increase with cluster size. However, the thermochemical stability or, in other words, the existence of a global minimum in the PES for C_5^{2+} and larger clusters is still an open question.

In this work we aim to investigate the stability and the electronic and vibrational properties of doubly charged carbon clusters up to $n = 9$. We provide geometries, absolute energies, dissociation energies and harmonic frequencies of the different species. Since a full inspection of the PES for these systems is beyond the scope of the present paper, we have only considered linear and cyclic conformations, and two different multiplicities (singlet and triplet) for each conformer. As shown in previous works,[11,12,16,29] these are the most stable structures for neutral and singly charged species, suggesting that this is likely the case for doubly charged carbon clusters.

The most recent theoretical works on neutral[11,12] and singly charged carbon clusters[29] show that, for these systems, geometries and harmonic frequencies obtained with various DFT methods are comparable to those obtained with coupled-cluster CCSD(T) methods. In the present work, we will use DFT to investigate doubly charged carbon clusters. Nevertheless, because there is no previous experience on these systems, we will also evaluate geometries and final energies at the CCSD(T) level as a further test of our computations. For a meaningful comparative study between the different neutral and charged species, we have also performed calculations for neutral and cationic species at the same level. This is also essential to obtain the first and second ionization potentials of the corresponding neutral parents

The paper is organized as follows. In the next section, we briefly summarize the computational methods we have used to perform the present study. In section 3, we present and discuss our results for the C_n^{2+} clusters and, when possible, we compare with the corresponding neutral and singly charged partners. We end the paper with some conclusions in section 4.

2. Computational Details

DFT calculations have been carried out by using the hybrid B3LYP functional. This DFT approach combines the Becke's three parameter non local hybrid exchange potential[47] with the non local correlation functional of Lee, Yang, and Parr.[48] The geometries of the different species under consideration have been optimized by using the 6-311+G(3df) basis set. To check convergence with the size of the basis set, we have performed geometry optimizations for C_n clusters with $n \leq 5$ using a smaller 6-31G(d) basis set. The bond lengths obtained with the latter basis differ by less than 0.01 Å in all cases.

The harmonic vibrational frequencies of the different stationary points of the PES have been calculated at the same level of theory than geometry optimizations in order to classify the stationary points of the PES as local minima or transition states (TS), and to estimate the corresponding zero point energies (ZPE). It is well established that, in general, both geometries and vibrational frequencies obtained at the B3LYP level are in fairly good agreement with experimental values.[49,50] In the particular case of small carbon clusters, previous theoretical studies have concluded that the calculated geometries and frequencies are very close to those obtained at the more expensive CCSD(T) level.[11,12,29] Nevertheless some caution must be exercised when using the DFT approach to describe small carbon clusters. C_2 and C_3^{2+} represent paradigmatic examples: in the first case DFT methods predict the $^3\Sigma_g^-$ state to be 53.6 kcal/mol more stable than the $^1\Sigma_g^+$ state, whereas high level ab initio calculations[51] predict the $^1\Sigma_g^+$ state to be the most stable one, in agreement with the experimental evidence. Something similar occurs in C_3^{2+} where, at DFT level, the triplet state is predicted to be more stable than the singlet, opposite to what is found in Multi Reference (MRDCI) calculations.[45] In both cases, it is well established that the ground state has a multiconfigurational character that explains the observed discrepancies.

To test the accuracy of the DFT calculations, we have reoptimized the geometries of the smaller C_n^{2+} clusters ($n \leq 5$) at the CCSD(T)/6-311G(2d) level (for n=5 this has been done only for linear conformers). Then, both B3LYP and CCSD(T) geometries are used to evaluate absolute energies at the CCSD(T)/6-311+G(3df) level. In the case of the B3LYP geometries, these CCSD(T) calculations are extended up to $n = 7$. In all DFT calculations we have also performed stability tests[52,53] to look for possible pathologies of the method. As a final test we have evaluated the mean value of S^2 to detect possible spin-contaminations. It is well described in the literature[54,55] that DFT calculations generally present lower spin contamination that HF-based methods, but, in those cases where spin contamination becomes large in DFT calculations, it can lead to spurious results for both geometries and energies.[54−57] All calculations have been performed by using the Gaussian-98 program.[58]

3. Results and Discussion

3.1 Stability and Accuracy of the DFT Calculations. The quality of the DFT calculations has been tested in two different ways: (a) by checking the stability of the DFT calculations and (b) by evaluating S^2 as a measure of spin contamination. In case (a), an analysis of the eigenvectors of the stability matrix[52] permits us to classify the instabilities as (*i*) restricted-unrestricted, R−U, when the transformations leading to a more stable solution only imply a change of spin multiplicity, (*ii*) internal, when those transformations only imply a change in orbital symmetry, and (*iii*) internal + R−U, when changes of both symmetry and multiplicity are involved. The results of these tests are reported in Table 1 together with the values of the energies and the zero point energy corrections. For the smaller systems, we also indicate the results of the CCSD(T)/6-311+G(3df) calculations performed using the B3LYP/6-311+G(3df) and CCSD(T)/6-311G(2d) geometries.

TABLE 1: Total Energies (*E* in a.u.), Zero Point Energy Corrections (ZPE, in a.u.), Relative Energies (ΔE in kcal/mol) and Mean Value of S^2 for All C_n^{2+} Clusters under Study

		B3LYP/6-311+G(3df)					CCSD(T)/6-311+G(3df)//B3LYP/6-311+G(3df)		CCSD(T)/6-311+G(3df)//CCSD(T)/6-311G(2d)	
	symmetry	E	ZPE	ΔE^b	S^2	DFT stability	E	ΔE^b	E	ΔE^b
C^{2+}	^1S	−36.51295		0.0		stable	−36.47833	0.0		
	^3P	−36.30448		130.8	2.000	stable	−36.23941	149.9		
C_2^{2+}	linear($D_{\infty h}$) $^1\Sigma_g^+$	−74.60848	0.00194	28.9		R−U	−74.49931	15.6	−74.49915	16.3
	linear($D_{\infty h}$) $^3\Sigma_g^-$	−74.65472	0.00213	0.0	2.005	internal	−74.52433	0.0	−74.52535	0.0
C_3^{2+}	linear($D_{\infty h}$) $^1\Sigma_g^+$	−112.82328	0.00681	45.5		internal + R−U	−112.69993	0.0	−112.70052	0.0
	linear($D_{\infty h}$) $^3\Sigma_u^+$	−112.89785	0.00892	0.0	2.011	stable	−112.66201	25.1	−112.66289	24.9
	cyclic(D_{3h}) $^1A'_1$	−112.88865	0.00915	5.9		R−U	−112.68580	10.3	−112.68784	9.4
	cyclic[a](C_{2v}) $^3A_1$	−112.87224	0.00654	14.6	2.048	stable	−112.63737	39.1	−112.63789	39.1
C_4^{2+}	linear($D_{\infty h}$) $^1\Sigma_g^+$	−151.05967	0.01093	0.0		R−U	−150.74568	6.1	−150.74594	5.9
	linear($D_{\infty h}$) $^3\Pi_g$	−151.02953	0.01302	20.2	2.046	internal	−150.70721	31.5	−150.70836	30.8
	cyclic(D_{4h}) $^1A_{1g}$	−151.02638	0.01086	20.8		R−U	−150.75528	0.0	−150.75531	0.0
	cyclic(D_{2h}) $^3B_{1u}$	−151.04355	0.01373	11.9	2.011	stable	−150.71755	25.5	−150.71819	25.1
C_5^{2+}	linear($D_{\infty h}$) $^1\Sigma_g^+$	−189.17307	0.01501	33.6		internal + R−U	−188.84744	0.0	−188.88000	0.0
	linear($D_{\infty h}$) $^3\Sigma_u^+$	−189.23202	0.02034	0.0	2.056	stable	−188.80718	28.8	−188.80769	48.7
	cyclic(C_{2v}) $^1A_1$	−189.12607	0.01892	65.6		stable	−188.75118	63.0		
	cyclic(C_{2v}) $^3B_2$	−189.13264	0.01786	60.8	2.013	stable	−188.7307	75.2		
C_6^{2+}	linear($D_{\infty h}$) $^1\Sigma_g^+$	−227.37883	0.02281	0.0		R−U	−226.88169	0.0		
	linear($D_{\infty h}$) $^3\Pi_u$	−227.33730	0.02418	26.9	2.067	internal	−226.83347	31.1		
	cyclic(D_{2h}) ^1A_g	−227.31939	0.02681	39.8		stable	−226.83455	32.1		
	cyclic(D_{3h}) $^3A'_2$	−227.32185	0.02635	38.0	2.111	stable	−226.81901	46.6		
C_7^{2+}	linear($D_{\infty h}$) $^1\Sigma_g^+$	−265.47394	0.02680	60.7		internal + R−U	−264.87503	71.7		
	linear($D_{\infty h}$) $^3\Sigma_u^+$	−265.50516	0.03099	43.8	2.087	stable	−264.89892	59.3		
	cyclic(D_{7h}) $^1A'_1$	−265.57761	0.03371	0.0		stable	−264.99618	0.0		
	cyclic(C_{2v}) $^3B_2$	−265.48939	0.02939	52.6	2.069	internal	−264.89213	62.6		
C_8^{2+}	linear($D_{\infty h}$) $^1\Sigma_g^+$	−303.65109	0.03376	0.0		stable				
	linear($D_{\infty h}$) $^3\Pi_g$	−303.60393	0.03936	33.1	2.088	internal				
	cyclic(D_{8h}) $^1A_{1g}$	−303.59476	0.05355	47.8		internal +R−U				
	cyclic(D_{8h}) $^3A_{2g:}$	−303.61902	0.04257	25.6	2.002	stable				
C_9^{2+}	linear($D_{\infty h}$) $^1\Sigma_g^+$	−341.73787	0.03764	6,8		internal + R−U				
	linear($D_{\infty h}$) $^3\Sigma_u^+$	−341.75006	0.04148	1,6	2.111	stable				
	cyclic(D_{9h}) $^1A'_1$	−341.72583	0.04063	16,3		internal + R−U				
	cyclic(C_{2v}) $^3A_2$	−341.74993	0,03882	0,0	2.0121	stable				

[a] Structure corresponds to a first-order transition state. [b] ZPE calculated at the B3LYP level of theory is included.

Table 1 reveals that, in some cases, the predicted relative energy between conformers are quite dependent on the level of theory used. In general, predictions of relative energies using DFT theory or CCSD(T) roughly differ by 10 kcal/mol, but, in some specific cases, as linear C_3^{2+} or linear C_5^{2+}, this value is larger than 50 kcal/mol, and the reverse energy ordering for the singlet and triplet structures is predicted with DFT compared to CCSD(T). It is important to notice that these cases correspond to situations where the DFT calculation predicts the triplet to be more stable than the singlet and where, more importantly, the DFT calculation for the singlet has an instability of the "internal + R−U" type (i.e., a lower energy can be obtained for the singlet by performing the calculation with an unrestricted DFT (UDFT) formalism). Although the stabilized UDFT solution leads to a lower value of the energy, a large mixing between the singlet and triplet configurations is obtained and the UDFT solution for the singlet presents a large spin contamination. For instance, for linear C_3^{2+} in a singlet configuration, the UDFT energy is −112.911 23 au, i.e., 0.1 au lower than that corresponding to the DFT calculation. However, the UDFT calculation leads to a wave function with $S^2 = 1.4$, instead of $S^2 = 0$ as it should be. Therefore, the stabilized (UDFT) solution does not represent an improvement of the DFT calculation. Thus the existence of R−U instabilities indicates that energy predictions obtained at DFT level must be taken with some caution. This analysis is especially useful for larger systems where CCSD(T) calculations are beyond our computational capabilities. Similar conclusions can be obtained when looking at internal instabilities. However, as for R−U instabilities, the resulting stabilized solutions present a very strong spin contamination and have a doubtful physical meaning.

In view of the previous discussion, it is crucial to analyze the reliability of the B3LYP geometries when the DFT calculations present instabilities. As shown in Table 2, B3LYP/6-311+G(3df) and CCSD(T)/6-311G(2d) calculations lead to similar structures (the differences are smaller than 0.03 Å) with the only exception of the linear singlet conformation of C_5^{2+}. Moreover the energies obtained at the CCSD(T)/6-311+G(3df) level using either the B3LYP or the CCSD(T) geometries are nearly identical. Table 1 shows that, in most cases, the absolute energies differ by less than 0.001 au and the relative stabilities by less that 1 kcal/mol. The only exception is the singlet linear conformation of C_5^{2+} whose stability is underestimated by 20 kcal/mol when using the B3LYP geometry. This is precisely a case that presents an "internal + R−U" instability at the DFT level. Therefore, DFT geometries associated with "internal + R−U" instabilities must be used with some caution, although the problem is much less severe than for energies.

Let us now analyze in more detail the problem of spin contamination obtained in some calculations. It can be seen in Table 1 that all the reported values present negligible spin contamination, but, in some regions of the PES, spurious minima showing large spin contamination can be obtained. For instance, in the case of linear C_4^{2+} with triplet multiplicity, the energy reported in Table 1 corresponds to a polyynic symmetric structure ($D_{\infty h}$) in which the bond distance r_{12} is equal to r_{34} (see also Table 2). The corresponding value of S^2 is 2.0459 which is very close to the theoretical value of 2. However, we

TABLE 2: C−C Distances (in Å) for All the Species Included in This Study Evaluated at the B3LYP/6-311+G(3df) Level

		linear clusters							
		r_{12}	r_{23}	r_{34}	r_{45}	r_{56}	r_{67}	r_{78}	r_{89}
C_2^{2+}	($D_{\infty h}$) $^1\Delta_g$	1.532 (1.557)							
	($D_{\infty h}$) $^3\Sigma_g^-$	1.501 (1.460)							
C_3^{2+}	($D_{\infty h}$) $^1\Sigma_g^+$	1.301 (1.289)	1.301 (1.289)						
	($D_{\infty h}$) $^3\Sigma_u^+$	1.269 (1.290)	1.269 (1.290)						
C_4^{2+}	($D_{\infty h}$) $^1\Sigma_g^+$	1.451 (1.459)	1.238 (1.255)	1.451 (1.459)					
	($D_{\infty h}$) $^3\Pi_g$	1.357 (1.383)	1.266 (1.276)	1.357 (1.383)					
C_5^{2+}	($D_{\infty h}$) $^1\Sigma_g^+$	1.415 (1.291)	1.282 (1.296)	1.282 (1.296)	1.415 (1.291)				
	($D_{\infty h}$) $^3\Sigma_u^+$	1.243 (1.258)	1.292 (1.298)	1.292 (1.298)	1.243 (1.258)				
C_6^{2+}	($D_{\infty h}$) $^1\Sigma_g^+$	1.385	1.236	1.347	1.236	1.385			
	($D_{\infty h}$) $^3\Pi_u$	1.310	1.262	1.309	1.262	1.310			
C_7^{2+}	($D_{\infty h}$) $^1\Sigma_g^+$	1.374	1.264	1.290	1.290	1.264	1.374		
	($D_{\infty h}$) $^3\Sigma_u^+$	1.232	1.304	1.266	1.266	1.304	1.232		
C_8^{2+}	($D_{\infty h}$) $^1\Sigma_g^+$	1.356	1.241	1.332	1.230	1.332	1.241	1.356	
	($D_{\infty h}$) $^3\Pi_g$	1.291	1.268	1.298	1.255	1.298	1.268	1.291	
C_9^{2+}	($D_{\infty h}$) $^1\Sigma_g^+$	1.351	1.259	1.295	1.272	1.272	1.295	1.259	1.351
	($D_{\infty h}$) $^3\Sigma_u^+$	1.350	1.262	1.294	1.274	1.274	1.294	1.260	1.350

		cyclic clusters								
		r_{12}	r_{23}	r_{34}	r_{45}	r_{56}	r_{67}	r_{78}	r_{89}	r_{91}
C_3^{2+}	(D_{3h}) $^1A'_1$	1.330 (1.364)	1.330 (1.364)	1.330 (1.364)						
	(C_{2v}) $^3A_1$	1.438 (1.460)	1.309 (1.330)	1.438 (1.460)						
C_4^{2+}	(D_{4h}) $^1A_{1g}$	1.442 (1.454)	1.442 (1.454)	1.442 (1.454)	1.442 (1.454)					
	(D_{2h}) $^3B_{1u}$	1.396 (1.412)	1.396 (1.412)	1.396 (1.412)	1.396 (1.412)					
C_5^{2+}	(C_{2v}) $^1A_1$	1.402	1.282	1.497	1.282	1.402				
	(C_{2v}) $^3B_2$	1.459	1.306	1.412	1.306	1.459				
C_6^{2+}	(D_{2h}) ^1A_g	1.355	1.293	1.292	1.356	1.292	1.293			
	(D_{3h}) $^3A'_2$	1.323	1.323	1.323	1.323	1.323	1.323			
C_7^{2+}	(D_{7h}) $^1A'_1$	1.291	1.291	1.291	1.291	1.291	1.291	1.291		
	(C_{2v}) $^3B_2$	1.309	1.278	1.329	1.434	1.329	1.278	1.309		
C_8^{2+}	(D_{8h}) $^1A_{1g}$	1.295	1.295	1.295	1.295	1.295	1.295	1.295	1.295	
	(D_{8h}) $^3A_{2g:}$	1.295	1.295	1.295	1.295	1.295	1.295	1.295	1.295	
C_9^{2+}	(D_{9h}) $^1A'_1$	1.291	1.291	1.291	1.291	1.291	1.291	1.291	1.291	1.291
	(C_{2v}) $^3A_2$	1.306	1.278	1.328	1.255	1.337	1.255	1.328	1.278	1.306

Values in brackets have been evaluated at the CCSD(T)/6-311G(2d) level.

have also found another minimum with energy −151.049 96 au, lower than the value reported in Table 1 and corresponding to an asymmetric cumulenic structure in which the three bond distances are different (1.290, 1.295, and 1.263 Å). In this case, $S^2 = 3.0378$, which shows that there is a strong spin contamination and, therefore, that this geometry must be discarded. An additional indication in favor of this argument is obtained by performing calculations[59] with exact eigenfunctions of S^2, i.e., with no spin contamination. This can be done by using either the Restricted Open-Shell Hartree−Fock (ROHF) formalism or a Restricted Open-shell CCSD(T) formalism based on a ROHF wave function (RHF−RCCSD(T)).[60] In both cases, by starting with an asymmetric structure as initial guess of the geometry optimization, we have found a global minimum associated to a symmetric structure very similar to that reported in Table 2 at the B3LYP level. Furthermore, by using a MRCDI method, Hogreve[46] has described a similar symmetric structure, with bond lengths 1.39 and 1.26 Å, which remains stable when symmetry constrains are removed. We have found similar asymmetric geometries in a few additional cases, but, as for C_4^{2+}, they present strong spin contamination and, therefore, they have been also discarded.

At this point it is worth analyzing if similar problems arise in neutral and singly charged carbon clusters. Most of the linear structures reported in reference[29] for singly charged C_n^+ clusters correspond to asymmetric geometries as those we have discarded for dications. We have found that minima corresponding to linear asymmetric C_n^+ clusters are always associated with an important spin contamination. This is due to the open-shell character of the singly charged species and to the proximity in energy of doublet and quartet states. As an illustration, let us consider the case of C_5^+. The most stable symmetric structure has an energy of −189.84263 au, while the most stable asymmetric structure has −189.86217 au (this structure is practically identical to that reported in reference[29]). However, the former gives $S^2 = 0.7625$, whereas the latter gives $S^2 = 0.8731$ (the exact value is 0.75). For this reason, in all our calculations of relative energies that will be presented below, we have chosen the linear symmetric structures. As for dications, the problem is much less important for neutral species than for cations. For instance, all the geometries reported by Martin et al.[11,12] for C_n clusters correspond to symmetric $D_{\infty h}$ structures. The explanation is simple. Neutrals and dications have an even number of electrons. In the case of closed electronic shells, restricted DFT calculations ensure the exact value $S^2 = 0$ for singlets. Triplet states are evaluated by performing unrestricted DFT calculations and, therefore, spin contamination with higher spin states is formally possible. However, triplet states are usually well separated in energy from higher spin states, which leads in practice to negligible or small spin contamination.

3.2 Structure. As already shown in Table 1, linear structures are the most stable ones for $n \leq 7$ except for C_4^{2+} and C_7^{2+}, which are cyclic. In the case of C_7^{2+}, the $^1A'_1$ state associated to a D_{7h} cyclic structure is the most stable one at both DFT and CCSD(T) levels by more than 50 kcal/mol with respect to the other three structures given in the table. However, for C_4^{2+}, the predictions of DFT and CCSD(T) calculations disagree. Although the DFT calculations lead to a linear singlet structure as the most stable one, CCSD(T) results predict the singlet cyclic structure to be the global minimum, very close in energy to the

linear singlet structure, in agreement with the conclusions of Hogreve[46] obtained at MRDCI level. Similar quasi-degeneracies between linear and cyclic structures have been described for the corresponding neutral[61−64] C_4 and cationic[29,62] C_4^+ clusters. For $n > 7$, where only DFT calculations have been performed, C_8^{2+} is predicted to have a global minimum associated to a linear singlet conformation with a much lower energy than that associated to other conformers. In the case of C_9^{2+}, the DFT results are not conclusive because the difference between the cyclic and the linear structures in their triplet states is only 1.6 kcal/mol, which is within the expected uncertainty of the DFT calculations. Moreover, the corresponding singlet structures lie only 6.8 and 16.3 kcal/mol above the global minimum, but both present "internal + R−U" instabilities and according to our previous discussion these structures might be more stable at higher levels of theory.

The C−C distances of the linear clusters under study have been summarized in Table 2. The first observation is that the structure of C_n^{2+} clusters is either cumulenic or polyynic. Clusters with singlet multiplicity present a polyynic character (except for C_5^{2+}) with terminal single bonds, whereas clusters with triplet multiplicity are cumulenic. This property does not change with cluster size. This is in contrast with the observations in neutral clusters because the latter are essentially cumulenic.[16] For C_n^+ cations,[29] there is an increase of the polyynic character with respect to neutral species, but without a clearly defined pattern as in the case of dications.

The polyynic character of the dications decreases with cluster size and, for the larger chains, the bond alternation tends to disappear. In the case of neutrals,[16] the bond alternation is only observed in C_4, whereas in the cations, the polyynic character is kept for larger clusters and the amplitude of the bond alternation is still large (0.040 Å) even for C_{12}^+. In the case of the dications, the polyynic character is more pronounced than in the cations. For instance, in C_8^{2+}, the difference between bonds is 0.111 Å, whereas for C_8^+, is 0.050 Å.[29]

The structure of cyclic species does not follow a simple pattern. With the exception of C_5^{2+} and C_6^{2+}, singlet states are associated to highly symmetric structures (D_{nh} for C_n^{2+} clusters), whereas triplet states exhibit, in general, a lower symmetry. Living apart the case of C_9^{2+}, which is ambiguous, the only cyclic structures associated with a global minimum appear for C_4^{2+} and C_7^{2+} in a singlet state. These clusters have D_{nh} symmetry and a cumulenic structure with double bonds similar to those found in linear clusters with triplet multiplicity. Polyynic cyclic structures appear less often and are less apparent than in linear species. The most remarkable example is the triplet state of C_5^{2+}, for which the bond lengths alternate as in linear polyynic species. In general, polyynic structures appear more frequently in cycles with an odd number of atoms and triplet multiplicity, which is in contrast with the behavior observed in linear species.

3.3 Dissociation Energies. In view of the recent experimental efforts to understand the fragmentation mechanisms of small positively charged clusters, we have evaluated the dissociation energies of C_n^{2+} dications corresponding to different fragmentation channels. Because dissociation energies are obtained as energy differences between the parent cluster and the various fragments, the absolute energies of neutral, cationic and dicationic species must be evaluated at the same level of theory. For neutral systems, accurate data exist,[16] but they have been obtained at a level of theory higher than that used in the present work. Thus, for consistency, we have evaluated the energies of neutral and singly charged species using the same B3LYP and CCSD(T) methods as for doubly charged species. It is important to point out that our calculated geometries and relative energies for neutral systems agree fairly well with the existing accurate data.

TABLE 3: Dissociation Energies (in eV) of the C_n^{2+} Clusters Calculated at the B3LYP Level of Theory

	$n-1$		
N	$C_n^{2+} \rightarrow C_{n-1}^{2+} + C$	$C_n^{2+} \rightarrow C_{n-1}^{+} + C^+$	$C_n^{2+} \rightarrow C_{n-1} + C^{2+}$
9	6.43	3.51	19.30
8	5.88	3.05	18.62
7	8.99 (8.83)	4.72 (4.80)	19.60 (18.74)
6	7.81 (6.72)	2.79 (2.29)	16.19 (15.36)
5	8.31 (8.41)	1.73 (2.16)	15.51 (15.61)
4	8.23 (7.40)	−0.48 (−0.56)	12.53 (12.02)
3	10.31 (10.66)	−1.21 (−0.64)	11.90 (11.88)
2	7.68 (7.20)	−5.81 (−5.84)	7.68 (7.20)
	$n-2$		
N	$C_n^{2+} \rightarrow C_{n-2}^{2+} + C_2$	$C_n^{2+} \rightarrow C_{n-2}^{+} + C_2^+$	$C_n^{2+} \rightarrow C_{n-2} + C_2^{2+}$
9	6.22	3.77	17.37
8	8.78	4.88	17.80
7	10.71 (9.56)	6.07 (5.66)	17.50 (16.99)
6	10.04 (9.14)	3.83 (3.42)	15.64 (15.13)
5	10.46 (9.83)	2.12 (2.38)	13.16 (13.23)
4	12.45 (12.08)	1.30 (1.30)	12.45 (12.08)
	$n-3$		
N	$C_n^{2+} \rightarrow C_{n-3}^{2+} + C_3$	$C_n^{2+} \rightarrow C_{n-3}^{+} + C_3^+$	$C_n^{2+} \rightarrow C_{n-3} + C_3^{2+}$
9	7.61	3.82	13.92
8	8.99	4.45	13.07
7	11.42 (10.72)	5.33 (4.93)	14.32 (13.30)
6	10.66 (9.29)	2.44 (1.78)	10.66 (9.29)
	$n-4$		
N	$C_n^{2+} \rightarrow C_{n-4}^{2+} + C_4$	$C_n^{2+} \rightarrow C_{n-4}^{+} + C_4^+$	$C_n^{2+} \rightarrow C_{n-4} + C_4^{2+}$
9	10.09	4.78	11.27
8	11.97	5.10	11.97

Numbers in brackets indicate dissociation energies calculated at the CCSD(T)/6-311+G(3df)//B3LYP/6-311+G(3df) level (see text).

Table 3 presents our results obtained both at the B3LYP and the CCSD(T) levels. We only report energies corresponding to dissociation of a given cluster in its most stable configuration (i.e., in the global minimum of the PES) leading to two fragments in their most stable configuration too. The difference between B3LYP and CCSD(T) calculations rarely exceeds 1 eV, being much smaller in most cases. It can be seen that the smallest carbon clusters, C_2^{2+}, C_3^{2+}, and C_4^{2+}, are thermodynamically unstable since, as expected, dissociation energies associated to the C_{n-1}^+/C^+ channels are negative. This is in agreement with the accurate theoretical predictions of Hogrevre,[45,46] who used multireference CI methods to evaluate the PES. Because these systems have been described in detail by this author, we will focus our discussion on the larger systems. We find that the smallest system that is stable against Coulomb explosion is C_5^{2+} in agreement with previous calculations.[44] The lowest dissociation energy corresponds to the C_4^+/C^+ channel, in agreement with the experimental results of Chabot et al.[39] who have found that this is the dominant fragmentation channel. Dissociation along this channel requires approximately 2 eV, i.e., ∼1 eV less than dissociation into C_3^+/C_2^+. All other channels have much higher dissociation energies. The third channel in increasing order of energy is $C_3^+/C^+/C$ (7.8 eV), which has also been observed experimentally.[39] Dissociation into these channels proceeds, most likely, through Coulomb barriers in the PES (because fragments are positively

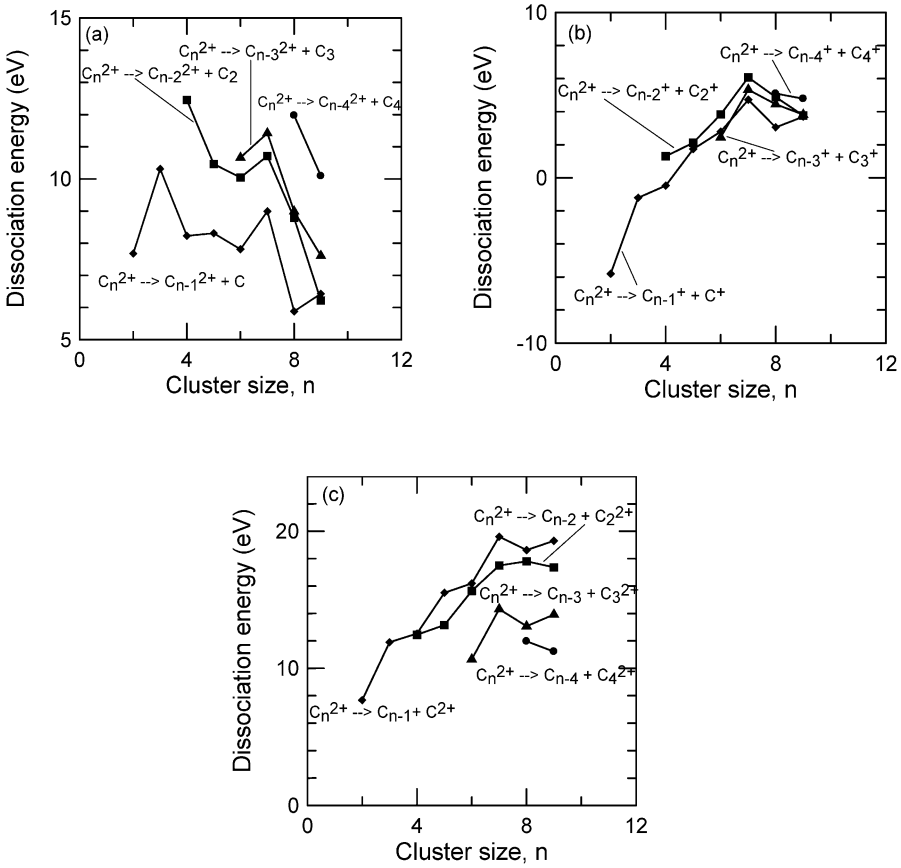

Figure 1. Dissociation energies (in eV) for the C_n^{2+} clusters. (a) Charge is carried by the biggest cluster fragment. (b) Charge is shared between both fragments. (c) Charge is carried by the smallest cluster fragment.

TABLE 4: First and Second Ionization Potentials (in eV) of Neutral C_n Clusters Calculated at the B3LYP Level of Theory

cluster	1st IP theoretical	1st IP experimental	2nd IP theoretical
C_1	11.55 (11.18)	11.26[h] (2nd IP 24.38[i])	25.04 (24.22)
C_2	11.92 (11.70)	11.41 ± 0.30[f],12.15[g]	23.07 (22.48)
C_3	12.03 (11.63)	12.97 ± 0.1[a], 12.6 ± 0.6[b], 12.1 ± 0.3[c]	20.25 (19.14)
C_4	11.26 (10.77)	12.54 ± 0.35[a], 12.6[b]	18.13 (17.42)
C_5	11.64 (11.15)	12.26 ± 0.1[a], 12.5 ± 0.1[b], 12.7 ± 0.5[d]	16.57 (15.61)
C_6	10.15 (10.28)	9.70 ± 0.2[a], 9.6 ± 0.3[e], 12.5 ± 0.3[d]	15.82 (15.21)
C_7	9.47	8.09 ± 0.1[e]	14.37
C_8	9.24	8.76 ± 0.1[e]	14.46
C_9	9.49	8.76 ± 0.1[e]	14.49

Numbers in brackets indicate ionization potentials calculated at the CCSD(T)/6-311+G(3df)//B3LYP/6-311+G(3df) level (see text). [a] Ref 34. [b] Ref 30. [c] Ref 33. [d] Ref 31. [e] Ref 32. [f] Ref 66. [g] Ref 67. [h] Ref 68. [i] Ref 69.

charged). Under this circumstance, dissociation may be so slow that some clusters may not have enough time to undergo fragmentation before they are detected. This may explain why the C_3^+/C_2^+ channel is less abundant than the $C_3^+/C^+/C$ one in the experiment.[39] Thus, the analysis of the experimental data cannot be exclusively based on thermodynamic stability but also requires the evaluation of the corresponding fragmentation rates.[65]

We show in Figure 1 the variation of dissociation energies with cluster size. It can be seen that, except for C_6^{2+}, the channel with the lowest dissociation energy is always $C_n^{2+} \rightarrow C_{n-1}^+ + C^+$, closely followed by $C_n^{2+} \rightarrow C_{n-3}^+ + C_3^+$ (which is, in fact, the lowest dissociation channel for C_6^{2+}). This is due to the strong stability of the C_3^+ cation; in particular, the extremely low dissociation energy of C_6^{2+} is due to the formation of two C_3^+ fragments. In general, channels in which each fragment carries a positive charge are energetically favored with respect to those leading to a neutral and a doubly charged fragment. Among the latter channels, those with the larger fragment carrying two positive charges are clearly favored. With a few exceptions, dissociation energies associated to C_{n-k}^+/C_k^+ and C_{n-k}/C_k^{2+} channels increase with cluster size for all k up to $n = 7$. In contrast, those associated to C_{n-k}^{2+}/C_k decrease or remain practically constant.

3.4 Ionization Potentials. Another interesting information that can be extracted from the present calculations is the first and second ionization potentials (IP) of neutral carbon clusters. The *adiabatic* IPs are shown in Table 4 and Figure 2, both at the B3LYP and CCSD(T) levels. Again, it can be observed that both sets of results are relatively close. In the case of the first ionization potentials, the differences never exceed 0.5 eV, whereas, in the case of the second ionization potentials, the differences are larger but they do not exceed 1 eV.

As a general trend, we can say that the first ionization potential slowly decreases with cluster size, but this decrease is not monotonic due to the presence of some oscillations. Adiabatic first ionization potentials have been previously evaluated by Giuffreda et al.[29] and measured by different

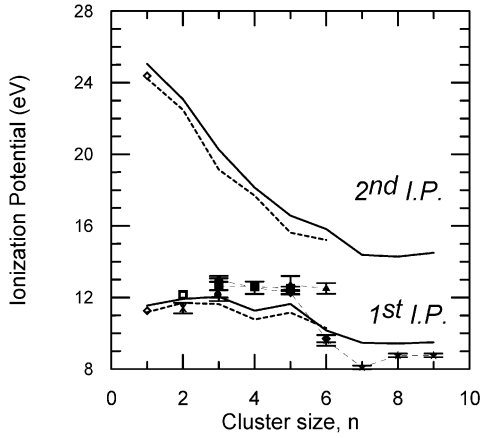

Figure 2. First and second ionization potentials for C_n clusters. Solid line: B3LYP/6-311+G(3df) level. Dashed line: CCSD(T)/6-311+G(3df)//B3LYP/6-311+G(3df) level. Experimental values are also included: diamonds (ref 34), squares (ref 30), circles (ref 33), triangles (ref 31), stars (ref 32), crosses (ref 66), open squares (ref 67), open diamonds (refs 68, 69) (see Table 4).

authors.[30−34,66−69] For comparison, experimental results are also included in Table 4 and Figure 2. Our results for C, C_2, C_3, and C_6 agree reasonably well with experiment, whereas those for C_4 and C_5 are approximately 1 eV lower than the experimental values and those for C_7, C_8, and C_9 are approximately 0.7 eV higher. In general, the variation of the IP's with cluster size and, in particular, the rapid decrease of the first IP around $n = 6$, is well reproduced by theory (see Figure 2). Reasonable agreement is also found when comparing with the values reported by Giuffreda et al.;[29] however, there are a few discrepancies that are worth analyzing in some detail. In particular, for C_5, our calculated value is 0.6 eV larger than that reported in reference.[29] As discussed in section 3.1, the most stable geometries of C_5 and C_5^+ showing minimum spin contamination correspond to doublet linear structures with symmetrical bonds with respect to the central carbon atom. However we have shown that, in the case of C_5^+, there is an asymmetric structure with lower energy but high spin contamination. It is the latter structure that Giuffreda et al.[29] actually used in their calculations. We have checked that, by using the energy associated to our calculated asymmetric structure, the ionization potential reduces to 11.1 eV, a value that is in excellent agreement with Giuffreda et al., but that is even farther from the experimental value. This fact reinforces the choice of symmetric structures in all our calculations and the argument that strong spin contamination is a useful criterion for rejection of some global minima at the DFT level. The discrepancy does not appear for C_4 or C_6 because the global minimum found by Giuffreda et al. for the corresponding ionic clusters correspond to symmetric linear structures.

In contrast with the first ionization potential, the second ionization potential decreases monotonically with cluster size. The observed behavior is quite predictable: the second IP is larger than the first IP and the difference between them is larger the smaller is the system. Except for atomic C, we are not aware of any experimental determination of the second IP to compare with.

3.5 Vibrational Frequencies. In Table 5, we show the harmonic frequencies calculated at the DFT level together with their symmetry. As is well-known, harmonic frequencies cannot be evaluated analytically when strong internal instabilities exist. For this reason, we only report this information in those cases where the DFT calculations are either stable or exclusively R−U unstable. These cases include the linear structures with the lowest energy at the DFT level and most of the cyclic structures (see instabilities in Table 1).

TABLE 5: Harmonic Frequencies (cm^{-1}) of C_n^{2+} Dications at the B3LYP/6-311+G(3df) Level

	(a) linear clusters
$C_2^{2+}\ ^1\Delta_g$	850(σ_g)
$C_3^{2+}\ ^3\Sigma_u^+$	213(π_u), 1321(σ_g), 2164(σ_u)
$C_4^{2+}\ ^1\Sigma_g^+$	129(π_u), 248(π_g), 793(σ_g), 1081(σ_u), 2164(σ_g)
$C_5^{2+}\ ^3\Sigma_u^+$	149(π_u), 275(π_g), 644(π_u), 807(σ_g), 1586(σ_u), 2132(σ_g), 2262(σ_u)
$C_6^{2+}\ ^1\Sigma_g^+$	88(π_u), 161(π_g), 329(π_u), 629(σ_g), 694(π_g), 1077(σ_u), 1400(σ_g), 2124(σ_u), 2233(σ_g)
$C_7^{2+}\ ^3\Sigma_u^+$	82(π_u), 192(π_g), 286(π_u), 553(π_g), 587(σ_g), 699(π_u), 1130(σ_u), 1701(σ_g), 2071(σ_u), 2230(σ_g), 2253(σ_u)
$C_8^{2+}\ ^1\Sigma_g^+$	59(π_u), 118(π_g), 190(π_u), 340(π_g), 495(σ_g), 592(π_u), 733(π_g), 920(σ_u), 1289(σ_g), 1511(σ_u), 2125(σ_g), 2197(σ_u), 2206(σ_g)
$C_9^{2+}\ ^3\Sigma_u^+$	52(π_u), 130(π_g), 218(π_u), 295(π_g), 461(σ_g), 506(π_u), 613(π_g), 735(π_u), 896(σ_u), 1303(σ_g), 1754(σ_u), 2080(σ_g), 2128(σ_u), 2218(σ_u), 2261(σ_g)
	(b) cyclic clusters
$C_3^{2+}(D_{3h})\ ^1A'_1$	1183(e′), 1652(a_1')
$C_3^{2+}(C_{2v})\ ^3A_1$	−1295(b_2), 1240(a_1), 1631(a_1)
$C_4^{2+}(D_{4h})\ ^1A_{1g}$	546(b_{2u}), 554(e_u), 633 (b_{1g}), 1232(b_{2g}), 1245(a_{1g})
$C_4^{2+}(D_{2h})\ ^3B_{1u}$	376(b_{3u}), 720(a_g), 811(b_{2u}), 1292(b_{3g}), 1384(a_g), 1444(b_{1u})
$C_5^{2+}(C_{2v})\ ^1A_1$	264(a_2), 367(b_1), 424(b_2), 739(a_1), 817(a_1), 1117(a_1), 1129(b_1), 1717(b_1), 1729(a_1)
$C_5^{2+}(C_{2v})\ ^3B_2$	316(b_2), 361(b_1), 430(a_2), 669(a_1), 734(b_1), 735(b_1),1200(a_1), 1657(b_1), 1735(a_1)
$C_6^{2+}(D_{2h})\ ^1A_g$	295(b_{2g}), 355(b_{1u}), 465(a_u), 505(a_g), 512(b_{2u}), 525(b_{1g}), 1153(b_{2u}), 1190(a_g), 1568(b_{2u}), 1669(b_{1g}), 1674(b_{3u}), 1853(a_g)
$C_6^{2+}(D_{3h})\ ^3A'_2$	431(a''_2), 438(e″), 552(e′), 642(a'_1), 1191(a'_1), 1252(e′), 1474(a'_2), 1671(e′)
$C_7^{2+}(D_{7h})\ ^1A'_1$	393(e'_1), 436(e''_1), 508(e'_1), 511(e''_1), 1113(a_1), 1376(e''_1), 1800(e''_1), 1818(e''_1)
$C_8^{2+}(D_{4h})\ ^3A_{2g}$	165(e_{1g}), 206(e_{1u}), 358(e_{1g}), 480(e_{1u}), 531(a_{1g}), 978(a_{1g}), 1226(e_{1u}), 1666(e_{1u}), 1676(e_{1g}), 2163(a_{2g}), 3463(a_{2u})
$C_9^{2+}(C_{2v})\ ^3A_2$[a]	23.8(b_2), 143.5 (b_2), 177.7(b_1), 236.7(a_2), 261.8(a_2), 264.9(b_1), 273.6(a_1), 399.2(b_1), 399.5(b_1), 477.6(b_2), 486.5(a_1), 526.5(a_1), 897.7(a_1), 1094.3(a_1), 1095.3(b_2), 1394.3(a_1), 1583.6(b_2), 1657.6(b_2), 1790.1(a_1)

[a] Frequencies calculated at the B3LYP/6-31G(d) level of theory.

4. Conclusions

In this work, we have studied the structure of small doubly charged carbon clusters using density functional (DFT) and coupled-cluster (CC) theories. Except for C_4^{2+} and C_7^{2+}, the most stable geometry corresponds to linear structures of $D_{\infty h}$ symmetry, which is at variance with neutral and singly charged carbon clusters. No definite conclusion can be obtained for C_9^{2+}. We have also discussed that DFT results can be affected by significant instabilities that must be carefully checked in order to avoid unphysical predictions of energies and frequencies. Nevertheless, in comparison with the more expensive CCSD(T) calculations, the DFT approach has been shown to be extremely useful in predicting accurate dissociation energies and ionization potentials. Except for C_6^{2+}, the channel with the lowest dissociation energy is always $C_n^{2+} \rightarrow C_{n-1}^+ + C^+$, closely followed by $C_n^{2+} \rightarrow C_{n-3}^+ + C_3^+$. With a few exceptions, dissociation energies associated with C_{n-k}^+/C_k^+ and C_{n-k}/C_k^{2+} channels increase with cluster size up to $n \approx 7$, whereas those associated with C_{n-k}^{2+}/C_k decrease or remain practically constant. Second ionization potentials decrease

monotonically with cluster size, in contrast with the first ionization potential, which presents some oscillations. Finally, we have provided the values of the harmonic frequencies which are useful in spectroscopy and for kinetic fragmentation studies.

Acknowledgment. We acknowledge Drs. M. Chabot, M. F. Politis and K. Wohrer for useful discussions. We also thank the CCC (*Centro de Computación Científica de la UAM*) for its generous allocation of computer time. This work has been supported by the *Dirección General de Investigación* (Spain), Project Nos. BQU2000-0245, BQU2001-0147, and BFM2000-0033.

References and Notes

(1) Van Orden, A.; Saykally, R. J. *Chem. Rev.* **1998**, *98*, 2313.
(2) Allamandola, L. J.; Hudgins, D. M.; Bauschlicher, C. W.; Langhoff, S. R. *Astron. Astrophys.* **1999**, *352*, 659.
(3) Lequeux, J.; Roueff, E. *Phys. Rep.* **1991**, *200*, 241.
(4) Roueff, E. *Bull. Soc. Fr. Phys.* **1997**, *109*, 7.
(5) Hinkle, K. W.; Keady, J. J.; Bernath, P. F. *Science* **1988**, *241*, 1319.
(6) Raghavachari, K.; Binkley, J. S. *J. Chem. Phys.* **1987**, *87*, 2191.
(7) Raghavachari, K.; Whiteside, R. A.; Pople, J. A. *J. Chem. Phys.* **1986**, *85*, 6623.
(8) Botschwina, P. *Theor. Chem. Acc.* **2000**, *104*, 160.
(9) Botschwina, P.; Schmatz, S. *Chem. Phys.* **1997**, *225*, 131.
(10) Schmatz, S.; Botschwina, P. *Chem. Phys. Lett.* **1995**, *235*, 5.
(11) Martin, J. M. L.; Elyazal, J.; Francois, J. P. *Chem. Phys. Lett.* **1995**, *242*, 570.
(12) Martin, J. M. L.; ElYazal, J.; Francois, J. P. *Chem. Phys. Lett.* **1996**, *252*, 9.
(13) Martin, J. M. L.; Francois, J. P.; Gijbels, R. *J. Chem. Phys.* **1990**, *93*, 8850.
(14) Martin, J. M. L.; Taylor, P. R. *Chem. Phys. Lett.* **1995**, *240*, 521.
(15) Martin, J. M. L.; Taylor, P. R. *J. Chem. Phys.* **1995**, *102*, 8270.
(16) Martin, J. M. L.; Taylor, P. R. *J. Phys. Chem.* **1996**, *100*, 6047.
(17) Radi, P. P.; Von Helden, G.; Hsu, M. T.; Kemper, P. R.; Bowers, M. T. *Int. J. Mass Spectrom. Ion Processes* **1991**, *109*, 49.
(18) Kemper, P. R.; Bowers, M. T. *J. Phys. Chem.* **1991**, *95*, 5134.
(19) Maier, J. P. *J. Phys. Chem. A* **1998**, *102*, 3462.
(20) O'Keefe, A.; Derai, R.; Bowers, M. T. *Chem. Phys.* **1984**, *91*, 161.
(21) Rohlfing, E. A. *J. Chem. Phys.* **1990**, *93*, 7851.
(22) Rohlfing, E. A.; Cox, D. M.; Kaldor, A. *J. Chem. Phys.* **1984**, *81*, 3322.
(23) Geusic, M. E.; Jarrold, M. F.; McIlrath, T. J.; Bloomfield, L. A.; Freeman, R. R.; Brown, W. L. *Z. Phys. D-Atoms Mol. Clusters* **1986**, *3*, 309.
(24) Geusic, M. E.; McIlrath, T. J.; Jarrold, M. F.; Bloomfield, L. A.; Freeman, R. R.; Brown, W. L. *J. Chem. Phys.* **1986**, *84*, 2421.
(25) McElvany, S. W.; Dunlap, B. I.; O'Keefe, A. *J. Chem. Phys.* **1987**, *86*, 715.
(26) McElvany, S. W. *J. Chem. Phys.* **1988**, *89*, 2063.
(27) Parent, D. C.; McElvany, S. W. *J. Am. Chem. Soc.* **1989**, *111*, 2393.
(28) Faibis, A.; Kanter, E. P.; Tack, L. M.; Bakke, E.; Zabransky, B. J. *J. Phys. Chem.* **1987**, *91*, 6445.
(29) Giuffreda, M. G.; Deleuze, M. S.; Francois, J. P. *J. Phys. Chem. A* **1999**, *103*, 5137.
(30) Drowart, J.; Burns, R. P.; DeMaria, G.; Inghram, M. G. *J. Chem. Phys.* **1959**, *31*, 1131.
(31) Dibeler, V. H.; Reese, R. M.; Franklin, J. L. *J. Am. Chem. Soc.* **1961**, *83*, 1813.
(32) Bach, S. B. H.; Eyler, J. R. *J. Chem. Phys.* **1990**, *92*, 358.
(33) Kohl, F. J.; Stearns, C. A. *J. Chem. Phys.* **1970**, *52*, 6310.
(34) Ramanathan, R.; Zimmerman, J. A.; Eyler, J. R. *J. Chem. Phys.* **1993**, *98*, 7838.
(35) Steger, H.; Devries, J.; Kamke, B.; Kamke, W.; Drewello, T. *Chem. Phys. Lett.* **1992**, *194*, 452.
(36) Lifshitz, C. *Int. J. Mass Spectrom.* **2000**, *200*, 423.
(37) Scheier, P.; Dunser, B.; Worgotter, R.; Muigg, D.; Matt, S.; Echt, O.; Foltin, M.; Mark, T. D. *Phys. Rev. Lett.* **1996**, *77*, 2654.
(38) Wohrer, K.; Chabot, M.; Rozet, J. P.; Gardes, D.; Vernhet, D.; Jacquet, D.; DellaNegra, S.; Brunelle, A.; Nectoux, M.; Pautrat, M.; LeBeyec, Y.; Attal, P.; Maynard, G. *J. Phys. B−At. Mol. Opt. Phys.* **1996**, *29*, L755.
(39) Chabot, M.; Wohrer, K.; Rozet, J. P.; Gardes, D.; Vernhet, D.; Jacquet, D.; DellaNegra, S.; Brunelle, A.; Nectoux, M.; Pautrat, M.; LeBeyec, Y. *Phys. Scr.* **1997**, *T73*, 282.
(40) Wohrer, K.; Fosse, R.; Chabot, M.; Gardes, D.; Champion, C. *J. Phys. B−At. Mol. Opt. Phys.* **2000**, *33*, 4469.
(41) Chabot, M.; Fosse, R.; Wohrer, K.; Gardes, D.; Maynard, G.; Rabilloud, F.; Spiegelman, F. *Eur. Phys. J. D* **2001**, *14*, 5.
(42) Wohrer, K.; Chabot, M.; Fosse, R.; Gardes, D.; Hervieux, P. A.; Calvayrac, F.; Reinhard, P. G.; Suraud, E. *Nucl. Instrum. Methods Phys. Res. Sect. B−Beam Interact. Mater. Atoms* **1998**, *146*, 29.
(43) Brechignac, C.; Cahuzac, P.; Carlier, F.; de Frutos, M. *Nucl. Instrum. Methods Phys. Res., Sect. B* **1994**, *88*, 91.
(44) Fosse, R. Ph.D. Thesis, 2000.
(45) Hogreve, H. *J. Chem. Phys.* **1995**, *102*, 3281.
(46) Hogreve, H. *J. Mol. Struct. (THEOCHEM)* **2000**, *532*, 81.
(47) Becke, A. D. *J. Chem. Phys.* **1993**, *98*, 5648.
(48) Lee, C.; Yang, W.; Parr, R. G. *Phys. Rev. B: Condens. Matter* **1988**, *37*, 785.
(49) Bauschlicher, C. W. *Chem. Phys. Lett.* **1995**, *246*, 40.
(50) Ziegler, T. *Chem. Rev.* **1991**, *91*, 651.
(51) Watts, J. D.; Bartlett, R. J. *J. Chem. Phys.* **1992**, *96*, 6073.
(52) Seeger, R.; Pople, J. A. *J. Chem. Phys.*, **1977**, *66*, 3045.
(53) Bauernschmitt, R.; Ahlrichs, R. *J. Chem. Phys.* **1996**, *104*, 9047.
(54) Wittbrodt, J. M.; Schlegel, H. B. *J. Chem. Phys.* **1996**, *105*, 6574.
(55) Ovchinnikov, A. A.; Labanowski, J. K. *Phys. Rev. A: At., Mol., Opt. Phys.* **1996**, *53*, 3946.
(56) Alcami, M.; Mo, O.; Yanez, M.; Cooper, I. L. *J. Chem. Phys.* **2000**, *112*, 6131.
(57) Goldstein, E.; Beno, B.; Houk, K. N. *J. Am. Chem. Soc.* **1996**, *118*, 6036.
(58) Frisch, M. J.; Trucks, G. W.; Schlegel, H. B.; Scuseria, G. E.; Robb, M. A.; Cheeseman, J. R.; Zakrzewski, V. G.; Montgomery, J. A., Jr.; Stratmann, R. E.; Burant, J. C.; Dapprich, S.; Millam, J. M.; Daniels, A. D.; Kudin, K. N.; Strain, M. C.; Farkas, O.; Tomasi, J.; Barone, V.; Cossi, M.; Cammi, R.; Mennucci, B.; Pomelli, C.; Adamo, C.; Clifford, S.; Ochterski, J.; Petersson, G. A.; Ayala, P. Y.; Cui, Q.; Morokuma, K.; Malick, D. K.; Rabuck, A. D.; Raghavachari, K.; Foresman, J. B.; Cioslowski, J.; Ortiz, J. V.; Stefanov, B. B.; Liu, G.; Liashenko, A.; Piskorz, P.; Komaromi, I.; Gomperts, R.; Martin, R. L.; Fox, D. J.; Keith, T.; Al-Laham, M. A.; Peng, C. Y.; Nanayakkara, A.; Gonzalez, C.; Challacombe, M.; Gill, P. M. W.; Johnson, B. G.; Chen, W.; Wong, M. W.; Andres, J. L.; Head-Gordon, M.; Replogle, E. S.; Pople, J. A. *Gaussian 98*, revision A3; Gaussian, Inc.: Pittsburgh, PA, 1999.
(59) Amos, R. D.; Bernhardsson, A.; Berning, A.; Celani, P.; Cooper, D. L.; Deegan, M. J. O.; Doobbyn, A. J.; Eckart, F.; Hampel, C.; Hetzer, G.; Knowles, P. J.; Korona, T.; Lindh, R.; Lloyd, A. W.; McNicholas, S. J.; Manby, F. R.; Meyer, W.; Mura, M. E.; Nicklass, A.; Palmieri, P.; Pitzer, R.; Rauhut, G.; Schütz, M.; Schumann, U.; Stoll, H.; Stone, A. J.; Tarroni, R.; Thorsteinsson, T.; Werner, H. J.; MOLPRO, a package of ab initio programs designed by H. J. Werner and P. J. Knowles ed., 2002.
(60) Watts, J. D.; Gauss, J.; Bartlett, R. J. *J. Chem. Phys.* **1993**, *98*, 8718.
(61) Martin, J. M. L.; Schwenke, D. W.; Lee, T. J.; Taylor, P. R. *J. Chem. Phys.* **1996**, *104*, 4657.
(62) Blanksby, S. J.; Schroder, D.; Dua, S.; Bowie, J. H.; Schwarz, H. *J. Am. Chem. Soc.* **2000**, *122*, 7105.
(63) Watts, J. D.; Gauss, J.; Stanton, J. F.; Bartlett, R. J. *J. Chem. Phys.* **1992**, *97*, 8372.
(64) Parasuk, V.; Almlof, J. *J. Chem. Phys.* **1991**, *94*, 8172.
(65) Hervieux, P. A.; Zarour, B.; Hanssen, J.; Politis, M. F.; Martin, F. *J. Phys. B: At., Mol. Opt. Phys.* **2001**, *34*, 3331.
(66) Reid, C. J.; Ballantine, J. A.; Andrews, S. R.; Harris, F. M. *Chem. Phys.* **1995**, *190*, 113.
(67) Huber, K. P.; Herzberg, G. *Molecular Spectra and Molecular Structure, 4: Constants of Diatomic Molecules*, 1979.
(68) Lide, D. R.; Editor *Handbook of Chemistry and Physics*, 77th ed.;, 1996.
(69) Kelly, R. L. *J. Phys. Chem. Ref. Data, Suppl.* **1987**, *16*, 1.